Synthesis, *in Vitro* and *in Silico* Studies of Some Novel 5-Nitrofuran-2-yl Hydrazones as Antimicrobial and Antitubercular Agents

Hatem Abdel-Kader Abdel-Aziz,*,[a,b] Wagdy Mohamed Eldehna,[c] Mohamed Fares,[c] Tilal Elsaman,[d] Marwa Mostafa Abdel-Aziz,[e] and Dalia Hussein Soliman[c,f]

[a] *Department of Pharmaceutical Chemistry, College of Pharmacy, King Saud University; P.O. Box 2457, Riyadh 11451, Saudi Arabia:* [b] *Department of Applied Organic Chemistry, National Research Center; Dokki, Cairo 12622, Egypt:* [c] *Department of Pharmaceutical Chemistry, Faculty of Pharmacy, Egyptian Russian University; Badr City, Cairo 11829, Egypt:* [d] *Department of Pharmaceutical Chemistry, College of Pharmacy, Omdurman Islamic University; P.O Box 382, Khartoum, Sudan:* [e] *The Regional Center for Mycology and Biotechnology, Al-Azhar University; Cairo 11759, Egypt: and* [f] *Pharmaceutical Chemistry Department, Faculty of Pharmacy (Girls), Al-Azhar University; Cairo 11754, Egypt.*
Received May 25, 2015; accepted June 21, 2015; advance publication released online July 8, 2015

In this study, we synthesized two series of novel 5-nitrofuran-2-carbohydrazides **21a–h** and **22a–e** in addition to a third series of thiophene-2-carbohydrazides **23a–g** to develop potent antimicrobial and/or antitubercular agents. The newly synthesized compounds were evaluated *in vitro* for their antimicrobial and antimycobacterial activities. Most of the 5-nitrofuran-2-carbohydrazides **21a–h** and **22a–e** displayed variable activity against *Aspergillus fumigates*, *Staphylococcus aureus*, *Streptococcus pneumonia*, *Bacillis subtilis*, *Salmonella typhimurium*, *Klebsiella pneumonia*, *Escherichia coli* and *Mycobacterium tuberculosis*. The sulfonamide derivative **21f** exhibited superior potency and broad-spectrum antimicrobial activity with minimum inhibitory concentration (MIC)=0.06–0.98 µg/mL and antimycobacterial activity with MIC=3.9 µg/mL. The 5-nitrofuran-2-carbohydrazides **21a, b, g, h** and **22a–c** exhibited significant antibacterial activity with MIC values in the range of 0.12–7.81 µg/mL. The significances of the 5-nitrofuran moiety and sulfonamide function were explored *via* the structure–activity relationship (SAR) study. In addition, docking studies revealed that the *p*-amino benzoic acid (PABA) and binding pockets of the dihydropteroate synthase (DHPS) were successfully occupied by compound **21f**. Furthermore, two quantitative structure–activity relationship (QSAR) models were built to explore the structural requirements which controlled the activity.

Key words synthesis; 5-nitrofuran; antimicrobial activity; antitubercular agent; quantitative structure–activity relationship (QSAR)

The Infectious Diseases Society of America, in 2010, underlined the urgent need of developing of new antibacterial drugs and it made a global commitment to develop ten novel antimicrobial agents before 2020.[1] This urgent response was due to the unacceptable high rate of morbidity and mortality of infectious diseases around the world in addition to the growing threat of antibiotic resistant pathogens.[2–4] Unfortunately, there is a drop in the number of authorization of new antimicrobial agents by the regulatory agencies and there is low probability to discover a novel lead compound in the preclinical studies.[5] On the other hand, most of the international pharmaceutical companies have been moving away from the area of antimicrobial discovery and the number of scientists involved in the search for novel broad antimicrobial leads was reduced dramatically.[6,7]

The discovery of the therapeutic potential of nitrofuran derivatives by Dodd and Stillman in 1944 during their research for antibacterial agents,[8] paved the way to design and synthesis various 5-nitrofuran analogs with a broad-spectrum activity against Gram-negative, Gram-positive bacteria and even some protozoa.[9] Although the mechanism of action of nitrofurans is not completely understood, previous studies accounted that under anaerobic conditions, the nitro group of the nitrofurans is reduced with formation of toxic free radical.[10] So, the incorporation of a nitro group at position 5 of furan ring resulted in a marked increase in antibacterial activity.[8] Nifuroxazide **1**, Nitrofurantoin **2**, Nifurtoinol **3**, Furazolidone

4, Nifuratel **5**, Nitrofural (Nitrofurazone) **6** and Nifurzide **7** (Fig. 1) are synthetic members of 5-nitrofuran hydrazone agents that used broadly in Europe, Africa, Middle East and India in the treatment of bacterial infections.[11–13] In addition, Nifurtimox **8** (Fig. 1) is often used to treat Chagas' disease which caused by *Trypanosoma cruzi*.[14] Although, some of the nitrofurans are not therapeutically employed due to their side effects,[15] there is a resurgence of interest in the in evaluation of novel nitroheterocycles as antimicrobials.[14,16–20]

Recently, several studies pointed out the importance of thiophene based derivatives as antibacterial agents.[21–23] Besides, Epimerox is a thiophene containing compound that prevented the growth of several Gram-positive pathogens.[24] Moreover, literature survey for functional groups which could be considered as pharmacophores for the antibacterial and antitubercular activities, revealed that the hydrazone moiety is common among many of the antibacterial drugs such as Nifuroxazide **1**[25] (Fig. 1). Moreover, isonicotinoyl hydrazide (INH) and its isonicotinoyl hydrazone analogs are well established antitubercular agents.[26–28]

Motivated by these findings, and in continuation of our ongoing interest in the synthesis and biological evaluation of different hydrazides and hydrazones as antimicrobial agents,[29,30] it was contemplated to synthesize new series of *N*-arylpropanehydrazonoyl chlorides derivatives of 5-nitrofuran **21a–h**, *N'*-(1-aryl/thiophenyl)-2-(phenylsulfonyl)ethylidene)-2-carbohydrazides of 5-nitrofuran **22a–e**, and *N*-arylpropane-
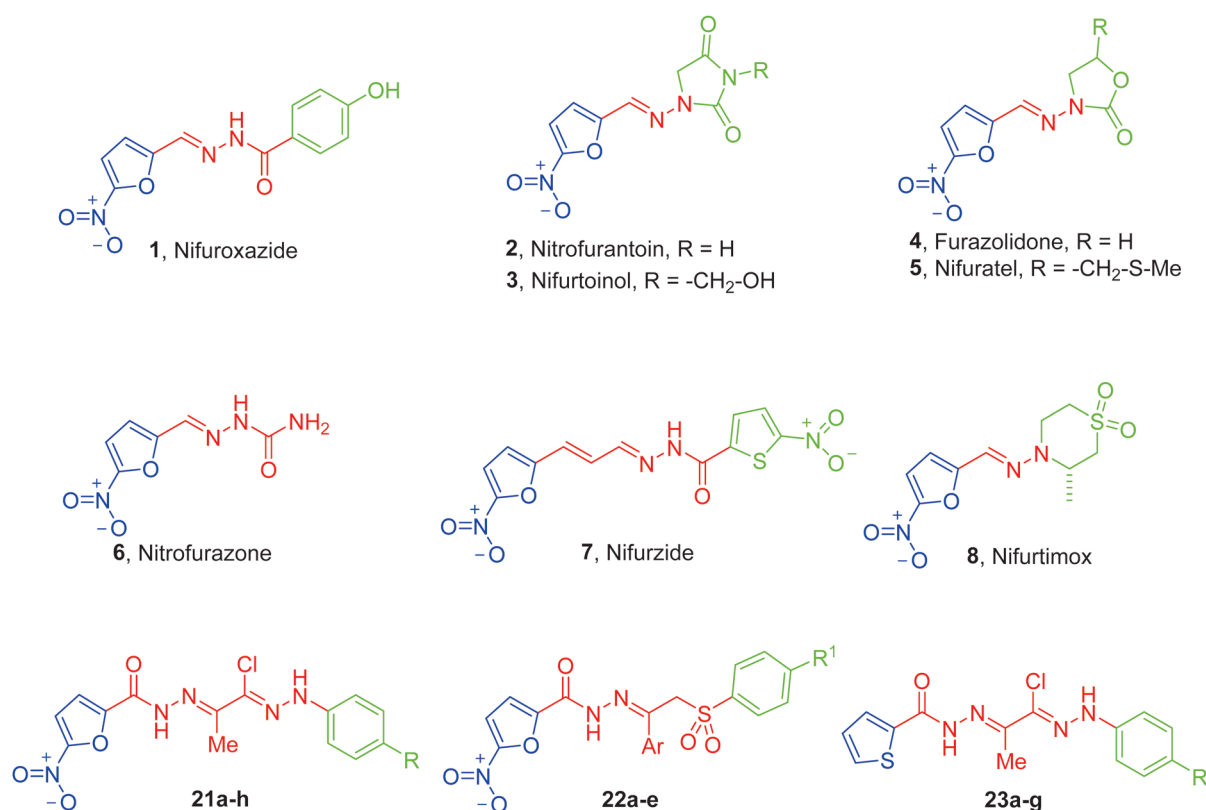
Fig. 1.   Structures of Some Antimicrobial 5-Nitrofurans **1–8** and the Targeted Compounds **21a–h**, **22a–e** and **23a–g**
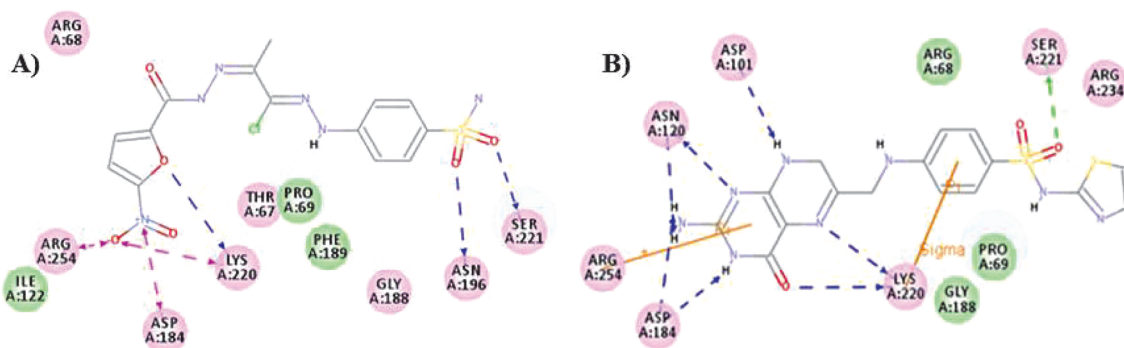

Fig. 2.   A) and B); 2D Representations of the Binding Patterns of **21f** and **STZ-DHPP** with BaDHPS Active Site
   PDB code 3TYE (STZ: sulfathiazole, DHPP: 6-hydroxymethyl-7,8-dihydropterin-pyrophosphate).

hydrazonoyl chlorides derivatives of thiophene **23a–g** with the prime aim of developing of potent antimicrobial and/or antitubercular agents. Furthermore, two-dimensional (2-D) quantitative structure–activity relationship (QSAR) models were generated to explore the structural requirements which controlled the different antimicrobial activities. Molecular docking studies were carried out to explain the significant results obtained by the most active compound.

RESULTS AND DISCUSSION

Discussion of Chemistry   In continuation of our endeavor towards the development of potent antimicrobial agents,[29–33] we synthesized a series of novel twenty 5-nitrofuran-2-carbohydrazide and thiophene-2-carbohydrazide derivatives bearing different aryl and heteroaryl rings. The synthetic route
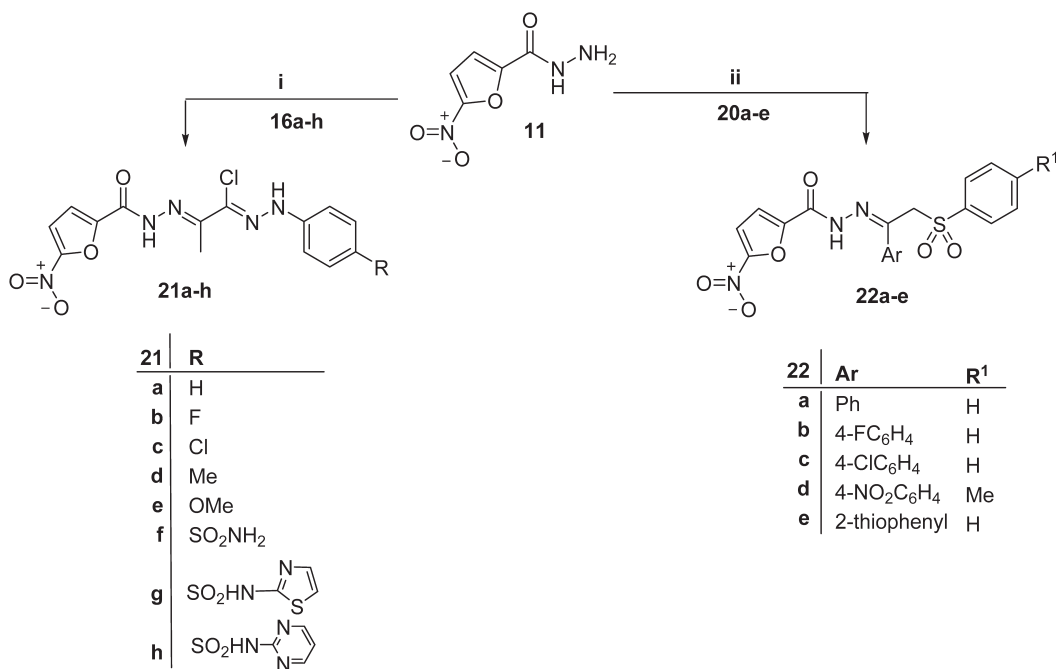
was initiated with the preparation of carbohydrazides **11** and **12**[34] (Chart 1). Diazotization of aromatic amines **13a–j** with hydrochloric acid and sodium nitrite gave diazonium salts **14a–j** which subsequently coupled with 3-chloropentane-2,4-dione (**15**) in ethanolic sodium acetate (Japp–Klingemann reaction) to afford oxo-*N*-arylpropanehydrazonoyl chlorides **16a–j**, respectively[35] (Chart 1). Moreover, bromination of ketones **17a–e** was performed using cupric bromide to yield the corresponding α-bromo ketones **18a–e**,[36] respectively, which then reacted with sodium benzenesulfinate (**19a**) or sodium toluenesulfinate (**19b**) to furnish the β-keto sulfones **20a–e**, respectively[37] (Chart 1).

Preparation of the target compounds **21a–h** was achieved *via* the reaction of the appropriate 2-oxo-*N*′-(4-substitutedphenyl)propanehydrazonoyl chloride **16a–h** with 5-nitrofuran-2-carbohydrazide **11** in refluxed tetrahydrofuran
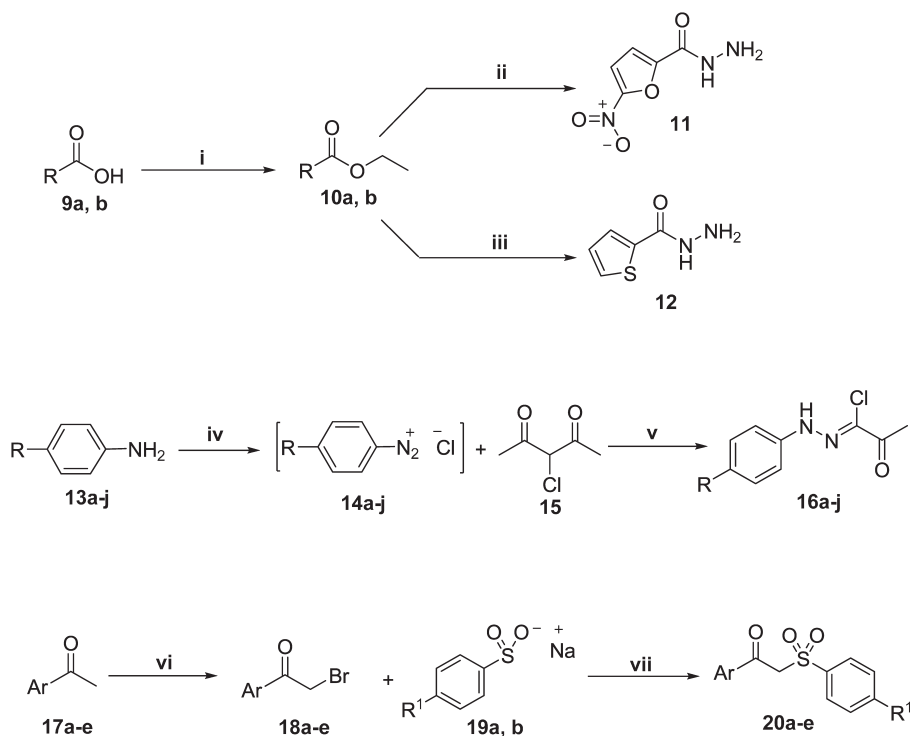
Reagents and conditions: **i**, EtOH/H$_2$SO$_4$/reflux 8 h; **ii**, NH$_2$NH$_2$·H$_2$O/EtOH/0–5°C/stirring 2 h; **iii**, NH$_2$NH$_2$·H$_2$O/EtOH/reflux 4 h; **iv**, HCl/NaNO$_2$/H$_2$O/0–5°C; (v), CH$_3$COONa/EtOH/0–5°C; **vi**, CuBr$_2$/CHCl$_3$/EtOAc; **vii**, EtOH/reflux 3 h.

Chart 1.   Synthesis of Compounds **11**, **12**, **16a–j** and **20a–e**

21	R
a	H
b	F
c	Cl
d	Me
e	OMe
f	SO$_2$NH$_2$
g	SO$_2$HN—(thiazolyl)
h	SO$_2$HN—(pyrimidinyl)

22	Ar	R^1
a	Ph	H
b	4-FC$_6$H$_4$	H
c	4-ClC$_6$H$_4$	H
d	4-NO$_2$C$_6$H$_4$	Me
e	2-thiophenyl	H

Reagents and conditions: **i**; THF/reflux 10 h. **ii**; Absolute ethyl alcohol/reflux 10 h.

Chart 2.   Synthesis of Compounds **21a–h** and **22a–e**

(THF) (Chart 2). Next, we aimed to hybride arylsulphone moiety, as promising class of antimicrobial agents,[38,39] with 5-nitrofuran scaffold through hydrazone linker. Thus, arylsulfones **20a–e** were condensed with 5-nitrofuran-2-carbohydrazide (**11**) in ethanol, in the presence of a catalytic amount of acetic acid, to give the corresponding arylsulphones **22a–e** (Chart 2).

Finally, different 2-oxo-*N*′-(4-substitutedphenyl)propane-hydrazonoyl chlorides were refluxed with thiophene-2-carbo-hydrazide (**12**) in THF to furnish the target derivatives **23a–g** (Chart 3).

IR spectra of bis-hydrazones **21a–h** and **23a–g** revealed the presence of stretching vibrations of the carbonyl groups in the region 1636–1696 cm^{-1}, in addition to the absorption bands of two NH functions in the region 32465–3481 cm^{-1}.

Also their ^{1}H-NMR spectra showed two D_2O exchangeable singlet signals in the regions δ 10.05–10.96 and 10.83–11.82 ppm attributable to two NH groups, in addition to the singlet signal of methyl group in the region δ 2.35–2.40 ppm. The sulfonamide **21f** and substituted sulfonamide **21g** and **21h** analogs displayed another D_2O exchangeable signal within 7.20–12.65 ppm. Compounds **21b–d**, **21f–h**, **23a–c** and **23e–g** were confirmed by their ^{13}C-NMR and showed a characteristic signal resonating at 152.00–188.62 ppm that confirmed the presence of carbonyl group. The analyses of the latter products

confirmed the assigned structure **21a–h** and **23a–g** (Charts 1, 2). Recently, we reported the X-ray diffraction structure for an analogue of compounds **21**, which confirmed the (1*Z*,2*E*)-configuration of these bis-hydrazones in solid state.[30]

On the other hand, structures of sulfones **22a–e** were characterized using their IR, ^{1}H-NMR, and MS spectra. The IR spectra of **22a–e** exhibited characteristic absorption band at 1680–1700 cm^{−1} due to C=O group, while that of the sulfonyl functionality was observed in the regions 1150–1158 cm^{−1} and 1307–1412 cm^{−1}. Their ^{1}H-NMR spectra exhibited the two

23	R
a	H
b	F
c	Cl
d	Br
e	I
f	Me
g	MeO
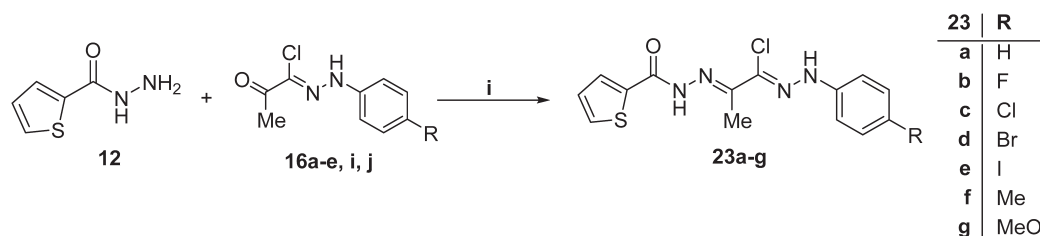
Reagents and conditions: **i**; THF/reflux 10 h.

Chart 3.   Synthesis of Compounds **23a–g**

Table 1.   Antimicrobial Activity of the Synthesized Compounds against the Pathological Organisms Expressed as Inhibition Diameter Zones in Millimeters (mm) Based on Well Diffusion Assay

Compd	Ar	R or R[1]	Fungi		Gram-positive bacteria			Gram-negative bacteria			
			Af	Ca	Sa	Sp	Bs	Pa	St	Kp	Ec
21a		H	18.3±0.58	NA	20.4±0.58	20.9±0.44	22.3±0.44	NA	20.3±0.58	21.6±0.37	19.6±0.58
21b		F	20.6±0.44	NA	20.4±0.35	21.2±0.44	22.3±0.25	19.2±0.25	20.6±0.37	22.4±0.63	20.3±0.63
21c		Cl	16.4±0.25	NA	NA	NA	NA	NA	NA	NA	NA
21d		Me	15.2±0.58	NA	16.2±1.2	17.1±0.58	17.9±2.1	NA	16.2±0.58	16.4±0.63	18.1±0.58
21e		OMe	14.6±0.63	NA	16.7±0.72	18.2±0.44	19.3±0.36	NA	17.4±0.58	19.3±0.63	16.2±0.58
21f		SO_2NH_2	22.3±0.58	NA	24.1±0.44	24.9±0.63	25.2±0.58	NA	21.4±0.37	22.6±0.63	21.3±0.63
21g		SO₂HN–thiazole	20.3±0.44	NA	21.6±0.63	23.8±1.2	23.9±0.44	NA	20.4±0.25	21.3±1.2	18.8±0.58
21h		SO₂HN–triazole	18.1±0.72	NA	20.2±0.72	18.6±0.58	21.8±0.58	NA	20.9±0.58	22.0±1.2	20.2±0.63
22a	Ph	H	16.3±0.25	NA	18.2±1.2	20.3±0.37	21.4±0.63	NA	20.3±0.48	21.2±0.63	18.5±0.58
22b	4-FC₆H₄	H	18.6±1.2	NA	20.4±1.2	22.3±0.63	22.4±0.58	NA	19.3±0.63	20.4±0.63	19.1±1.2
22c	4-ClC₆H₄	H	17.2±1.2	NA	19.3±0.63	18.1±0.58	21.2±0.72	NA	20.1±0.58	21.0±0.63	19.2±0.58
22d	4-NO₂C₆H₄	CH3	13.2±1.2	NA	15.1±0.44	16.2±0.44	16.9±0.72	NA	15.1±0.58	15.9±0.72	13.1±1.2
22e	2-Thiophenyl	H	NA	NA	NA	NA	NA	NA	NA	NA	NA
23a		H	NA	NA	NA	NA	NA	NA	NA	NA	NA
23b		F	NA	NA	NA	NA	NA	NA	NA	NA	NA
23c		Cl	17.2±0.72	NA	NA	NA	NA	NA	NA	NA	NA
23d		Br	NA	NA	NA	NA	NA	NA	NA	NA	NA
23e		I	NA	NA	NA	NA	NA	NA	NA	NA	NA
23f		Me	NA	NA	NA	NA	NA	NA	NA	NA	NA
23g		OMe	NA	NA	NA	NA	NA	NA	NA	NA	NA
AB			20.4±0.24	21.6±0.22							
CF					20.2±0.34	20.3±0.58	20.4±0.14	19.1±0.15	19.8± 0.63	19.7±0.12	20.3± 0.44

NA: No activity. The screening organisms, Mould: *Aspergillus fumigatus* (RCMB 02568, An), An Yeasts: *Candida albicans* (RCMB 05036, Ca), Gram-positive bacteria: *Staphylococcus aureus* (RCMB 010028, Sa), *Streptococus pneumoniae* (RCMB 010010, Sp), and *Bacillus subtilis* (RCMB 010069, Bs). Gram-negative bacteria: *Pseudomonas aeruginosa* (RCMB 010043, Pa), *Salmonella typhimurium* (RCMB 010315, St), *Klebsiella penumoniae* (RCMB 0010093, Kp) and *Escherichia coli* (RCMB 010052, Ec), AB: Amphotericin B, CF: Ciprofloxacin.

Table 2.   Antimicrobial Activity as MICs (μg/mL) of Tested Standards and Synthesized Compounds against Tested Microorganisms

Compd	Fungi		Gram-positive bacteria			Gram-negative bacteria			
	Af	Ca	Sa	Sp	Bs	Pa	St	Kp	Ec
21a	7.81	NA	**1.95**	**0.98**	**0.49**	NA	**1.95**	**0.98**	3.90
21b	**0.98**	NA	**1.95**	**0.98**	**0.49**	**3.90**	**0.98**	**0.49**	**1.95**
21c	NA	NA	NA	NA	NA	NA	NA	NA	NA
21d	62.5	NA	31.25	15.63	7.81	NA	31.25	31.25	7.81
21e	62.5	NA	15.63	7.81	3.90	NA	7.81	**3.90**	31.25
21f	**0.49**	NA	**0.12**	**0.06**	**0.06**	NA	**0.98**	**0.24**	**0.98**
21g	**1.95**	NA	**0.49**	**0.12**	**0.12**	NA	**1.95**	**0.98**	3.90
21h	7.81	NA	**1.95**	3.90	**0.49**	NA	**0.98**	**0.49**	**1.95**
22a	31.25	NA	7.81	**1.95**	**0.98**	NA	**1.95**	**0.98**	3.90
22b	3.90	NA	**1.95**	**0.49**	**0.49**	NA	**1.95**	**1.95**	3.90
22c	15.63	NA	3.90	7.81	**0.98**	NA	**1.95**	**0.98**	3.90
22d	125	NA	62.50	31.25	15.63	NA	62.50	31.25	125
22e	NA	NA	NA	NA	NA	NA	NA	NA	NA
23a	NA	NA	NA	NA	NA	NA	NA	NA	NA
23b	NA	NA	NA	NA	NA	NA	NA	NA	NA
23c	15.63	NA	NA	NA	NA	NA	NA	NA	NA
23d	NA	NA	NA	NA	NA	NA	NA	NA	NA
23e	NA	NA	NA	NA	NA	NA	NA	NA	NA
23f	NA	NA	NA	NA	NA	NA	NA	NA	NA
23g	NA	NA	NA	NA	NA	NA	NA	NA	NA
AB	1.95	0.49							
CF			1.95	1.95	1.95	3.90	3.90	3.90	1.95

NA: No Activity. Results in bold indicate more or equal activity relative to standard drugs. The screening organisms, Mould: *Aspergillus fumigatus* (RCMB 02568, An), An Yeasts: *Candida albicans* (RCMB 05036, Ca), Gram-positive bacteria: *Staphylococcus aureus* (RCMB 010028, Sa), *Streptococus pneumoniae* (RCMB 010010, Sp), and *Bacillus subtilis* (RCMB 010069, Bs). Gram-negative bacteria: *Pseudomonas aeruginosa* (RCMB 010043, Pa), *Salmonella typhimurium* (RCMB 010315, St), *Klebsiella penumoniae* (RCMB 0010093, Kp) and *Escherichia coli* (RCMB 010052, Ec), AB: Amphotericin B, CF: Ciprofloxacin.

D_2O-exchangeable signal of hydrazone NH at δ 11.13–11.67 ppm. The compounds **22c–e** showed characteristic ^{13}C-NMR signal at δ 181.77–189.03 ppm attributed to the carbonyl group.

Discussion of Anti-microbial Activity Antibacterial, antifungal and antimycobacterial activities were performed at The Regional Center for Mycology and Biotechnology (RCMB), Al-Azhar University, Cairo, Egypt.

Anti-fungal Activity Target compounds **21a–h**, **22a–e**, **23a–g** and amphotericin, a membrane-active polyene macrolide antibiotic and an antifungal reference drug,[40] were evaluated *in vitro* for their antifungal activity by inhibition zone technique and minimum inhibitory concentration (MIC). Data in Tables 1 and 2 revealed that all the compounds showed no activity against *Candida albicans*, while compounds **21b**, **f**, **g** and **22b** showed a remarkable activity against *Aspergillus fumigatus*.

Aspergillus fumigatus is largely responsible for increasing the mortality rate in immunocompromised patients due to invasive aspergillosis (IA).[41] The main reason for this unacceptable mortality rate is the limited number of antifungal agents.[42] Whilst, the thiophene containing counterparts **22e** and **23a–g** displayed no activity, the 5-nitrofuran derivatives **21a–h** and **22a–d** showed moderate to excellent activity toward the *Aspergillus fumigatus* with MIC values ranging from 0.49 to 125 μg/mL. In particular, the sulfonamide derivative **21f** was found to be the most potent counterpart against *Aspergillus fumigatus* organism (MIC=0.49 μg/mL) as it was four times more active than the reference drug Amphotericin B (MIC=1.95 μg/mL).

Antimycobacterial and *in Vitro* Cytotoxic Activities

Antitubercular activity of the newly synthesized derivatives **21a–h**, **22a–e** and **23a–g** against *M. tuberculosis* (RCMB 010126) was evaluated at The Regional Center for Mycology and Biotechnology (RCMB), Al-Azhar University, Cairo, Egypt. The mean values of the inhibition zone diameter and the minimum inhibitory concentrations were listed in Table 3. Isoniazide and pyrazinamide were included in the experiments as reference drugs (MIC=0.40 and 3.21 μg/mL, respectively).

Analysis of the data in Table 3 illustrated that compounds of the first series **21a–h** and second series **22a–e** displayed good to fair antimycobacterial activity, while the third series derivatives **23a–g** lacked the activity, in a similar fashion to the antifungal and antibacterial activities. Compound **21f**, which possessed superior antifungal and antibacterial activities, exploited the most potent antitubercular activity (I.Z=19.6±0.58 mm and MIC=3.90 μg/mL), confirming the significance of the incorporation of the sulfonamido functionality. In addition, compounds **21a**, **b**, **g**, **h** and **22a–c** showed moderate antitubercular activity with MIC values ranging from 7.81 to 31.25 μg/mL.

In vitro cytotoxicity of the most active antimicrobial and antitubercular compounds **21a**, **f–g** and **22a–c** was evaluated against human breast MDA-MB-231 cells using 3-(4,5-dimethylthiazol-2-yl)-2,5-diphenyltetrazolium bromide (MTT) method. Doxorubicin was used as the positive control drug. The IC_{50} values obtained for these compounds are listed in Table 3. None of the tested compounds displayed any significant cytotoxicity, thereby providing a high therapeutic index. Selectivity index (SI) is used to estimate the therapeutic effect of a drug and to identify drug candidates for further studies. SI

Table 3. Anti-tubercular (MIC), Cytotoxicity (IC$_{50}$) and Selectivity Index (SI) of the Synthesized Compounds

Compd	I.Z	MIC$^{a)}$	IC$_{50}$$^{b)}$	SI$^{c)}$
21a	17.6±0.37	7.81	>50	>6.4
21b	16.3±0.58	31.25	n.d.	n.d.
21c	NA	NA	n.d.	n.d.
21d	14.3±1.2	125	n.d.	n.d.
21e	15.2±0.58	62.50	n.d.	n.d.
21f	19.6±0.58	3.90	>50	>12.8
21g	18.1±0.58	7.81	>50	>6.4
21h	17.1±0.58	15.63	33.70±0.03	2.16
22a	17.2±1.4	15.63	>50	>3.2
22b	17.6±0.44	7.81	>50	>6.4
22c	16.6±0.73	15.63	>50	>3.2
22d	14.3±0.63	125	n.d.	n.d.
22e	NA	NA	n.d.	n.d.
23a	NA	NA	n.d.	n.d.
23b	NA	NA	n.d.	n.d.
23c	NA	NA	n.d.	n.d.
23d	NA	NA	n.d.	n.d.
23e	NA	NA	n.d.	n.d.
23f	NA	NA	n.d.	n.d.
23g	NA	NA	n.d.	n.d.
Isoniazide		**0.40**		
Pyrazinamide		**3.21**		
Doxorubicin			**0.31±0.09**	

a) Minimum inhibitory concentration of *M. tuberculosis* (μg/mL). *b)* Measurement of cytotoxicity in breast MDA-MB-231 cells: 50% inhibitory concentrations (μg/mL). *c)* Selectivity index (*in vitro*): IC$_{50}$ in breast MDA-MB-231/MIC against *M. tuberculosis*. NA: No Activity, n.d.: not determined.

of each compound was determined as the ratio of IC$_{50}$ to MIC (Table 3). It was reported that, new drugs candidates must have SI equal or higher than 1.[43] In this study, **21f** could be considered as a promising new anti-tubercular drug candidate with SI >12.8.

Antibacterial Activity Initially, all the synthesized compounds (**21a–h**, **22a–e** and **23a–g**) were evaluated *in vitro* for their antibacterial activity, by inhibition zone technique, using three Gram-positive bacteria that are *Staphylococcus aureus* (RCMB 010028), *Streptococus pneumoniae* (RCMB 010010), and *Bacillus subtilis* (RCMB 010069) and four Gram-negative bacteria that are *Pseudomonas aeruginosa* (RCMB 010043), *Salmonella typhimurium* (RCMB 010315), *Klebsiella penumoniae* (RCMB 0010093) and *Escherichia coli* (RCMB 010052), as presented in Table 1. Subsequently, MIC of all the synthesized compounds was evaluated *in vitro* using the two-fold serial dilution technique. The lowest concentration showing no growth was taken as the MIC. The results of minimum inhibitory concentration were reported in Table 2. Ciprofloxacin, a broad-spectrum widely used antibacterial and the most potent marketed fluoroquinolone against Gram-negative bacteria,[12] was used as reference drug in this assay.

As shown in Tables 1 and 2, the tested compounds displayed different levels of antibacterial activity and possessed a distinctive pattern of selectivity against the tested strains. With the exception of compounds **21c** and **22e**, all compounds of the first and second series showed a remarkable broad-spectrum antibacterial activity against almost all tested strains used in the assay. On the other hand, the remaining compounds **23a–g** had no significant activity against any of the

tested strains at concentration up to 125 μg/mL. All the tested Gram-positive and Gram-negative strains were susceptible to the all active compounds influence, except *P. aeruginosa* affected only with compound **21b**. Investigation of the activity against *B. subtilis* indicated that it was the most sensitive strain to the influence of the active members.

Observing the results, we could deduce valuable data about the structure activity correlation of the tested compounds. Firstly, we explored the impact of substitution of the 4-position of the pendant phenyl group in the first series compounds **21a–h**. Incorporation of unsubstituted phenyl group led to compound **21a** with broad and excellent activity against *S. aureus*, *S. pneumonia*, *B. subtilis*, *S. typhimurium*, *K. pneumonia* and *E. coli* (MIC=0.49–3.9 μg/mL). Since fluorine has a size and electronic properties similar to those of hydrogen, it is introduced as an isosteric to the hydrogen atom. Compound **21b** bearing fluorine substituent at the 4-position, showed an increase in the activity against the tested Gram-negative bacteria, especially against *P. aeruginosa* (MIC=3.9 μg/mL). Also, it retained the activity of the Gram-positive one suggesting that the substitution in the 4-position may be tolerated also suggesting that the halogens incorporation may be advantageous. Conversely, substitution with more bulky chlorine atom, compound **21c**, abolished the activity. Furthermore, grafting methyl group, compound **21d**, and methoxy group, compound **21e**, resulted in drop of the activity (MIC=3.9–31.25 μg/mL).

Concerning the effect of the substitution in the first series member's **21a–e**, the activities were decreased in the order of 4-F>unsubstituted>4-OMe>4-Me>>>4-Cl, hinting that grafting a small electron-withdrawing group like fluorine is more beneficial than an electron-donating group like methyl or methoxy for the antibacterial activity.

Taking into consideration the importance of sulfonamido substituent as antimicrobial pharmacophore,[44] 4-sulfonamido functionalities were incorporated in **21f–g** counterparts. Unsubstituted sulfonamide derivative **21f** emerged as the most potent analog with outstanding antimicrobial activities (MIC=0.06–0.98 μg/mL), confirming the importance of sulfonamido substitution. Notably, **21f** analog displayed more susceptibility towards Gram-positive bacteria (MIC=0.06–0.12 μg/mL) more than Gram-negative one (MIC=0.24–0.98 μg/mL), relative to the standard drug. Substitution with more bulky sulfonamide derivatives *N*-(thiazol-2-yl)sulfonamido and *N*-(pyrimidin-2-yl)sulfonamido produced compounds **21g** and **h** with potent and broad-spectrum activity (MIC=0.12–3.9 μg/mL), respectively. Thence, the order of activities of the sulfonamides members in the first series, were decreased in the order of sulfanilamide>sulfathiazole>sulfadiazine for the Gram-positive strains, and in the order of sulfanilamide>sulfadiazine>sulfathiazole for the Gram-positive bacteria. Moreover, a molecular docking study was used to explain the obtained excellent biological data of **21f**.

Considering the activities of 5-nitrofuran analogs containing sulfone group **22a–e**, 4-F substituted analog **22b** exhibited superior activity against Gram-positive bacteria (*S. aureus*, *S. pneumonia* and *B. subtilis*) with MIC values of 1.95, 0.49 and 0.49 μg/mL, respectively, confirming the particularity of the incorporation of small electron-withdrawing group. In addition, the unsubstituted **22a** and the 4-Cl substituted **22c** derivatives elicited good antibacterial activity against the

Table 4. Docking Scores of the Tested Compound and STZ

Compound	CDOCKER energy (kcal/mol)	CDOCKER interaction energy (kcal/mol)
21f	−39.265	−52.744
STZ	−47.276	−63.925

Table 5. Toxicity Risks Evaluation of Novel 5-Nitro Furan Hydrazones

	Mutagenicity	Developmental toxicity potential	Skin irritation potential
21a	0.11	0	0
21b	0	0	0
21c	0.34	0	0
21d	0.17	0	0
21e	0.14	0	0
21f	0	0	0
21g	0	0.72	0
21h	0	0.61	0
22a	0	0	0
22b	0	0	0
22c	0	0	0

tested strains (MIC=0.98–7.81 μg/mL). On the other hand, compound **22d** possessed modest activity against the tested bacteria (MIC=15.63–125 μg/mL). Also, it was found that the replacement of the phenyl group with 2-thiophenyl one, as compound **22e**, led to complete loss of activity.

Interestingly, bioisosteric replacement of the 5-nitrofuran moiety with thiophene one in the third series led up to diminished activity, confirming the role of 5-nitrofuran group as a crucial element for the antibacterial activity.

DISCUSSION OF *IN SILICO* STUDIES

Docking Study It is well known that, the sulfonamides exert their antimicrobial activity through competition with *p*-amino benzoic acid (PABA) substrate for the DHPS enzyme active site and thus inhibiting the biosynthesis of dihydrofolic acid.[45] Crystallographic data of *Bacillus anthracis* dihydropteroate synthase (BaDHPS) bound to sulfathiazole-6-hydroxymethyl-7,8-dihydropterin-pyrophosphate (STZ-DHPP) adduct was obtained from Protein Data Bank (PDB code 3TYE).[46]

Similarly, data obtained from docking shows that **21f** can interact with BaDHPS as STZ-DHPP with the same target. The benzene-sulfonamide moiety of **21f** occupies virtually the same position observed in the STZ-DHPP-BaDHPS complex; thereby establishing the characteristic hydrogen bond between its sulfonamide moiety and the backbone NH group of Ser221, in addition to an extra hydrogen bond with Asn196 (Fig. 2). Concerning the PABA binding pocket, the 5-nitro furan moiety of compound **21f** extends into the pteridine-binding pocket establishing hydrogen bond between the side chain of Lys220 and the oxygen of furan ring and another ionic bond between −NO$_2$ and the side chain of Lys220. Although, the pteridine ring itself forms a hydrogen bond with the side chain of Asp184, the same amino acid forms ionic bond with nitrogen of 5-nitro furan (Fig. 2). Moreover, CDOCKER interaction scores—compared to STZ—gave us precious results that may

justify the superior biological activity of **21f** (Table 4).

Toxicity Risk Assessment Screening As indicated in Table 5 toxicity risk assessment screening showed that only compounds **21a**, **c**, **12d** and **21e** have low risk of mutagenicity on prolonged usage whereas compounds **21g** and **h** exhibited risk of developmental toxicity. All the tested compounds have not showed any risk of irritation. It is noteworthy that the most active compound **21f** showed no risk of tumorogenicity, developmental toxicity or reproductive toxicity.

2D QSAR Study

Development of QSAR Models

The establishment of quantitative relationships between structural features and measured bioactivities, QSAR, is one of the most useful strategies in the quest for new bioactive molecules. Thus, QSAR models were built with the objective of analyzing and correlating the physicochemical and biological behaviors of the newly synthesized compounds. The analysis was run by means of the DS 2.5 software (Discovery Studio 2.5, Accelrys, Co., Ltd.).

A set of the active members (**21a–h** and **22a–d**) was used as a training set with their measured pMIC against *Bacillis subtilis* and *Mycobacterium tuberculosis* for QSAR modeling.

Various molecular properties of the training set compounds were calculated *via* the "Calculate Molecular Properties" module. 2D Descriptors involved: A log*P*, Finger prints, molecular properties, molecular property counts, surface area and volume and topological descriptors, while the 3D descriptors involved: Dipole, jurs descriptors, principle moments of inertia, shadow indices and surface area and volume. Genetic function approximation (GFA) was adopted to search for the best possible QSAR regression equation capable of correlating the variations in the biological activities of the training compounds with variations in the generated descriptors, *i.e.*, multiple linear regression modeling (MLR). QSAR models were validated employing leave one-out cross-validation by setting the folds to a number much larger than the number of samples, r^2 (squared correlation coefficient value) and r^2 prediction (predictive squared correlation coefficient value), residuals between the predicted and experimental activity of the test set and training set.

QSAR Study Results

Equation 1 represents the best performing QSAR model for the activity against *Bacillis subtilis*:

$$-\log \text{MIC} = 4.0948 + 0.8749\,\textbf{CHI\_V\_3\_P}$$
$$+ 0.3273\,\textbf{IAC\_Total}$$
$$- 0.1476\,\textbf{Molecular\_Volume}. \quad (1)$$

Equation 2 represents the best performing QSAR model for the activity against *Mycobacterium tuberculosis*:

$$-\log \text{MIC} = 5.2719 - 0.8597\,\textbf{ES\_Count\_aasC}$$
$$- 0.4935\,\textbf{Jurs\_RNCS}. \quad (2)$$

According to Eqs. 1 and 2, the QSAR models were represented graphically by scattering plots of the experimental *versus* the predicted bioactivity values–log MIC for the training set compounds as shown in Figs. 3 and 4. The method used to build the model was least-squares, r^2=0.871 and 0.772, respectively, r^2 (**adj**)=0.822 and 0.722, respectively, r^2 (**pred**)=0.754 and 0.570 respectively, least-squared error=0.1026 and 0.0619,
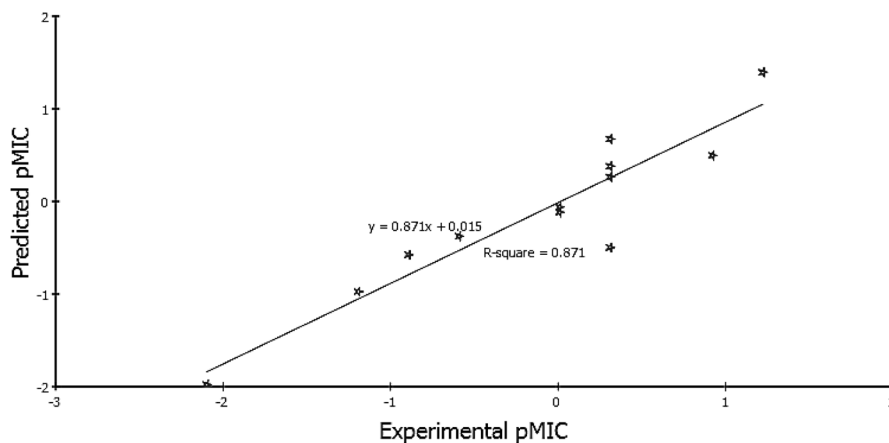
Fig. 3. Predicted *versus* Experimental pMIC of the Tested Compounds against *Bacillis subtilis* According to Eq. 1 ($r^2=0.871$)
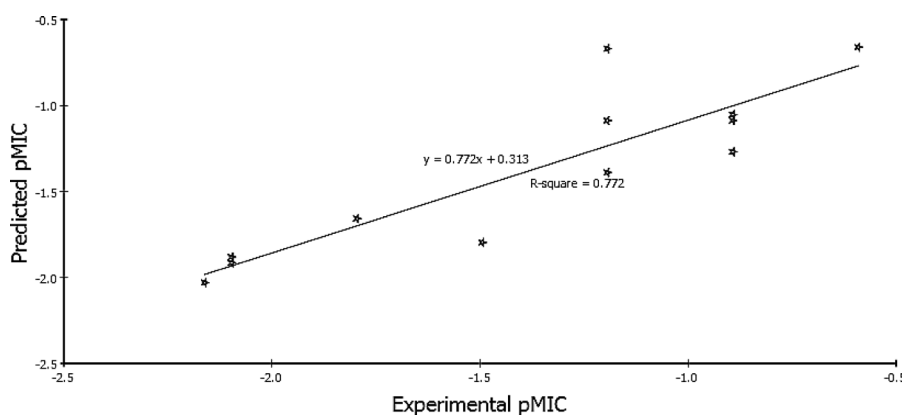

Fig. 4. Predicted *versus* Experimental pMIC of the Tested Compounds against *M. tuberculosis* According to Eq. 2 ($r^2=0.772$)

respectively, where r^2 (adj) is r^2 adjusted for the number of terms in the model; r^2 (pred) is the prediction r^2, equivalent to q^2 from a leave-1-out cross-validation.

In conclusion, Eq. 1 suggested that antibacterial activity of the 5-nitrofuran derivatives **21a–h** and **22a–d** towards *Bacillus subtilis* is affected by the topological descriptors (**CHI_V_3_P** and **IAC_Total**) and the molecular volume. CHI_V (Kier & Hall valence-modified connectivity index), a 2-D topological descriptor, is a refinement of the molecular connectivity index where a vertex subgraph valence delta is enhanced to delta *v* to take into account electron configuration of the atom represented by the vertex: $\delta^v=(Z^v-h/Z-Z^v-1)$ where *v* is the number of valence electrons in the atom, *Z* is its atomic number, and *h* is the number of hydrogens bound to it. This formula is designed to reproduce the unmodified molecular connectivity index for saturated hydrocarbons, for which delta *v*=delta. However, delta *v* distinguishes between multiple and single bonds. The denominator introduces further distinction between element rows due to the presence of the atomic number.[47,48] IAC_Total (Total Information of Atomic Composition) is a graph-theoretical infoContent topological descriptor that helps to differentiate molecules according to their size, degree of branching, flexibility, and overall shape using graph-theory concepts.[49]

On the other hand Eq. 2 indicated that antimycobacterial activity of the 5-nitrofuran derivatives **21a–h** and **22a–d** is affected by the estate keys (**ES_Count_aasC**) and the Jurs (**Jurs_RNCS**) descriptors. Estate keys calculate the sums of

the electrotopological state (E-state) values and/or the counts of each atom type.[50,51] ES_Count_aasC calculates the E-state count for carbon with two aromatic bonds and one single bond. Moreover, Jurs descriptors are those ones that combine shape and electronic information to characterize molecules.[52] The descriptors are calculated by mapping atomic partial charges on solvent-accessible surface areas of individual atoms. Jurs_RNCS (relative negative charge surface area) is the solvent-accessible surface area of most negative atom divided by the relative negative charge.

QSAR Validation

Robustness of the established QSAR models 1 and 2 was verified by using; Leave-one-out (LOO) internal validation ($r^2=0.871$ and 0.772, respectively). Cross-validation was also employed where q^2, which is equivalent to r^2 (**pred**), was 0.754 and 0.570, respectively. In addition, validation was employed by measuring the residuals between the experimental and the predicted activities of the training set (Tables 4, 5). Interestingly, the predicted activities by the QSAR models were very close to those experimentally observed, indicating that these models could be applied for prediction of more effective hits having the same skeletal framework.

CONCLUSION

In the present investigation, initially, we synthesized the 5-nitrofuran hydrazides **21a–h** and **22a–e** and evaluated their antimicrobial and antimycobacterial activities. Amphotericin

Table 6. Experimental Activity of the Synthesized Derivatives against the Predicted Activity and Calculated Descriptors Governing Activity According Eq. 1

Compd	Experimental activity (−log MIC)	Predicted activity (−log MIC)	Residual	CHI_V_3_P	IAC_Total	Molecular_Volume
21a	0.3098	−0.4982	0.808	3.03	70.19	204.77
21b	0.3098	0.3802	−0.0704	3.1	75.15	210.25
21c	−2.0969	−1.9788	−0.1182	3.36	73.15	223.29
21d	−0.8927	−0.5763	−0.3164	3.31	74.61	216.77
21e	−0.5911	−0.3763	−0.2148	3.35	77.75	222.6
21f	1.2219	1.394	−0.1722	4.37	87.23	237.69
21g	0.9208	0.4953	0.4255	6.25	101.12	285.71
21h	0.3098	0.2642	0.0456	5.56	101.95	285.03
22a	0.0088	−0.0604	0.0691	5.47	80.64	239.41
22b	0.3098	0.6737	−0.3639	5.54	85.94	246.61
22c	0.0088	−0.1184	0.1271	5.79	85.94	253.47
22d	−1.194	−0.9744	−0.2196	6.05	92.68	275.77

Table 7. Experimental Activity of the Synthesized Derivatives against the Predicted Activity and Calculated Descriptors Governing Activity According Eq. 2

Compd	Experimental activity (−log MIC)	Predicted activity (−log MIC)	Residual	ES_Count_aasC	Jurs_RNCS
21a	−0.8927	−1.0877	0.1951	3	7.6602
21b	−1.4949	−1.7959	0.3011	4	7.3530
21c	−2.1614	−2.0299	−0.1315	4	7.8271
21d	−2.0969	−1.9143	−0.1827	4	7.5928
21e	−1.7959	−1.6574	−0.1385	4	7.0724
21f	−0.5911	−0.6608	0.0697	4	5.0529
21g	−0.8927	−1.0534	0.1607	5	4.1063
21h	−1.1940	−1.0878	−0.1061	5	4.1761
22a	−1.1940	−0.6694	−0.5246	4	5.0703
22b	−0.8927	−1.2696	0.3770	5	4.5445
22c	−1.1940	−1.3900	0.1960	5	4.7883
22d	−2.0969	−1.8807	−0.2162	6	4.0405

B and Ciprofloxacin were used as references for antifungal and antibacterial screening, while, Isoniazid and Pyrazinamide were used as references for antimycobacterial activity. The results evidenced that all the compounds displayed moderate to excellent activity except **21c** and **22e**. Amongst the active compounds, the sulfonamide derivative **21f** displayed the best activity against *A. fumigatus* and panel of three Gram-positive bacteria, four Gram-negative bacteria and *M. tuberculosis* (MIC=0.06–3.9 μg/mL) relative to the reference drugs. Based on the activities of many thiophene containing antimicrobials, we synthesized and biologically evaluated **23a–g** as potential antimicrobial and antimycobacterial agents. Unfortunately, all the thiophene hydrazides **23a–g** were devoid of activity, confirming the role of 5-nitrofuran group as a crucial element for the antibacterial activity. Moreover, toxicity risk assessment screening and evaluation of selective index demonstrated the safety and high therapeutic index of **12f** counterpart. QSAR models were established *via* the Discovery Studio 2.5 software in order to identify positive and negative structural features within the 5-nitrofuran derivatives. Finally, molecular docking studies indicated that compound **21f** could occupy both PABA and pterin binding pockets of the dihydropteroate synthase (DHPS), suggesting that it could act by the inhibition of microbial DHPS enzyme in addition to the formation of toxic free radical reported in 5-nitro furan derivatives. The

attractive results demonstrated the potential and importance of developing novel 5-nitrofuran-2-carbohydrazide counterparts to treat fungal, bacterial and mycobacterial infections.

MATERIALS AND METHODS

General Chemistry Melting points (mp) were measured with a Stuart melting point apparatus and were uncorrected. The NMR spectra were recorded by Varian Gemini-300BB 300MHz FT-NMR spectrometers (Varian Inc., Palo Alto, CA, U.S.A.). [1]H and ^{13}C spectra were run at 500 and 125MHz, respectively, in deuterated dimethyl sulfoxide (DMSO-d_6). Chemical shifts (δ_{H}) are reported relative to tetramethylsilane, as internal standard. Electron impact mass spectra were measured on a Varian MAT 311-A (70 eV). Reaction courses and product mixtures were routinely monitored by thin layer chromatography (TLC) on silica gel precoated F$_{254}$ Merck plates. Unless otherwise noted, all solvents and reagents were commercially available and used without further purification.

Synthesis of Hydrazones 21a–h To a stirred solution of the 5-nitrofuran-2-carbohydrazide **11** (5 mmol), 2-oxo-*N′*-(4-substitutedphenyl)propanehydrazonoyl chloride **16a–h** (5 mmol) was added in THF (30 mL). The reaction mixture was heated under reflux for 10h. The solid product obtained upon cooling was filtered off and recrystallized from dioxan

to afford the corresponding hydrazones **21a–h** with 65–80% yield.

(1Z,2E)-2-(2-(5-Nitrofuran-2-carbonyl)hydrazono)-N′-phenylpropanehydrazonoyl Chloride (21a) Orange powder (yield 75%), mp 230°C; IR (KBr, *v* cm⁻¹): 3414, 3315 (2NH), 1668 (C=O) and 1599 (C=N); ¹H-NMR (DMSO-d_6) δ ppm: 2.38 (s, 3H, CH₃), 6.94–7.98 (m, 7H, ArH), 10.27 (s, D₂O exch., 1H, =NNH–), 11.10 and 11.55 (s, D₂O exch., 1H, –CONH–); MS *m/z* [%]: 351 [(M+2)⁺, 9.3], 349 [M⁺, 26.9], 92 [100].

(1Z,2E)-N′-(4-Fluorophenyl)-2-(2-(5-nitrofuran-2-carbonyl)hydrazono)propanehydrazonoyl Chloride (21b) Orange powder (yield 75%), mp 232°C; IR (KBr, *v* cm⁻¹): 3420, 3317 (2NH), 1652 (C=O) and 1589 (C=N); ¹H-NMR (DMSO-d_6) δ ppm: 2.36 (s, 3H, CH₃), 7.13 (t, *J*=7.5 Hz, 2H, Ar-H), 7.36–7.97 (m, 4H, ArH), 10.29 (s, D₂O exch., 1H, =NNH–), 11.10 and 11.54 (s, D₂O exch., 1H, –CONH–); ¹³C-NMR (DSMO-d_6) δ ppm: 19.02, 113.48, 115.66 (³J_{F-C}=7.5 Hz), 116.11(²J_{F-C}=22.5 Hz), 122.15, 123.50, 127.00, 140.46 (2C), 152.53, 156.83 (¹J_{F-C}=236.3 Hz), 157.41; MS *m/z* [%]: 369 [(M+2)⁺, 7.0], 367 [M⁺, 18.9], 110 [100].

(1Z,2E)-N′-(4-Chlorophenyl)-2-(2-(5-nitrofuran-2-carbonyl)hydrazono)propanehydrazonoyl Chloride (21c) Red powder (yield 75%), mp 231°C; IR (KBr, *v* cm⁻¹): 3414, 3319 (2NH), 1669 (C=O) and 1595 (C=N); ¹H-NMR (DMSO-d_6) δ ppm: 2.36 (s, 3H, CH₃), 7.35–7.96 (m, 6H, ArH), 10.39 (s, D₂O exch., 1H, =NNH–), 11.15 and 11.56 (s, D₂O exch., 1H, –CONH–); ¹³C-NMR (DSMO-d_6) δ ppm: 13.88, 113.47, 115.94, 122.13, 125.32, 129.46, 142.86, 146.91, 152.56, 147.33, 148.81, 154.89; MS *m/z* [%]: 387 [(M+4)⁺, 1.4], 385 [(M+2)⁺, 8.3], 383 [M⁺, 12.6], 126 [100].

(1Z,2E)-2-(2-(5-Nitrofuran-2-carbonyl)hydrazono)-N′-p-tolylpropanehydrazonoyl Chloride (21d) Red powder (yield 75%), mp 239°C; IR (KBr, *v* cm⁻¹): 3420, 3315 (2NH), 1668 (C=O) and 1576 (C=N); ¹H-NMR (DMSO-d_6) δ ppm: 2.25 (s, 3H, CH₃), 2.35 (s, 3H, CH₃), 7.10 (d, *J*=6 Hz, 2H, Ar-H), 7.24 (d, *J*=6 Hz, 2H, Ar-H), 7.68–7.97 (m, 2H, H³ and H⁴ of furan), 10.17 (s, D₂O exch., 1H, =NNH–), 11.09 and 11.52 (s, D₂O exch., 1H, –CONH–); ¹³C-NMR (DSMO-d_6) δ ppm: 13.82, 20.76, 113.47, 114.39, 115.32, 122.43, 130.02, 141.57, 146.47, 147.11, 147.40, 152.49, 157.40; MS *m/z* [%]: 365 [(M+2)⁺, 9.8], 363 [M⁺, 28.8], 106 [100].

(1Z,2E)-N′-(4-Methoxyphenyl)-2-(2-(5-nitrofuran-2-carbonyl)hydrazono)propanehydrazonoyl Chloride (21e) Brown powder (yield 75%), mp 224°C; IR (KBr, *v* cm⁻¹): 3414, 3318 (2NH), 1668 (C=O) and 1576 (C=N); ¹H-NMR (DMSO-d_6) δ ppm: 2.35 (s, 3H, CH₃), 3.73 (s, 3H, OCH₃), 6.90 (d, 2H, Ar-H, *J*=7.5 Hz), 7.29 (d, 2H, Ar-H, *J*=7.5 Hz), 7.70–7.98 (m, 2H, H³ and H⁴ of furan), 10.13 (s, D₂O exch., 1H, =NNH–), 11.10 and 11.51 (s, D₂O exch., 1H, –CONH–); MS *m/z* [%]: 381 [(M+2)⁺, 3.5], 379 [M⁺, 10.2], 122 [100].

(1Z,2E)-2-(2-(5-Nitrofuran-2-carbonyl)hydrazono)-N′-(4-sulfamoylphenyl)propanehydrazonoyl Chloride (21f) Red powder (yield 75%), mp 260°C; IR (KBr, *v* cm⁻¹): 3390–3264 (2NH,NH₂), 1670 (C=O) and 1596 (C=N); ¹H-NMR (DMSO-d_6) δ ppm: 2.37 (s, 3H, CH₃), 7.20 (s, D₂O exch., 2H, SO₂NH₂), 7.46 (d, *J*=7.5 Hz, 2H, Ar H), 7.75–7.95 (m, 4H, ArH), 10.59 (s, D₂O exch., 1H, =NNH–), 11.14 and 11.57 (s, D₂O exch., 1H, –CONH–); ¹³C-NMR (DSMO-d_6) δ ppm: 19.00, 113.98, 115.01, 122.20, 125.29, 127.74, 136.75, 138.19, 145.66, 152.51, 157.46, 188.56; MS *m/z* [%]: 456

[(M+2)⁺, 4.6], 454 [M⁺, 11.8], 105 [100]; MS *m/z* [%]: 430 [(M+2)⁺, 1.2], 428 [M⁺, 3.0], 64 [100].

(1Z,2E)-2-(2-(5-Nitrofuran-2-carbonyl)hydrazono)-N′-(4-(N-thiazol-2-ylsulfamoyl)phenyl)propanehydrazonoyl Chloride (21g) Orange powder (yield 75%), mp 233°C; IR (KBr, *v* cm⁻¹): 3419–3253 (3NH), 1682 (C=O) and 1597 (C=N); ¹H-NMR (DMSO-d_6) δ ppm: 2.38 (s, 3H, CH₃), 6.82 (d, *J*=3 Hz, 1H, H⁵ of thiazole), 7.25 (d, *J*=3 Hz, 1H, H⁴ of thiazole), 7.45 (d, *J*=7.5 Hz, 2H, Ar-H), 7.54-7.96 (m, 4H, ArH), 10.63 (s, D₂O exch., 1H, =NNH–), 10.96 and 11.61 (s, D₂O exch., 1H, –CONH–), 12.65 (s, D₂O exch., 1H, SO₂NH-); ¹³C-NMR (DSMO-d_6) δ ppm: 25.90, 108.41, 113.50, 114.01, 115.04, 124.86, 125.14, 127.99, 134.77, 136.24, 145.90, 146.74, 153.50, 156.00, 188.57; MS *m/z* [%]: 511 [M⁺, 0.1], 111 [100].

(1Z,2E)-2-(2-(5-Nitrofuran-2-carbonyl)hydrazono)-N′-(4-(N-pyrimidin-2-ylsulfamoyl)phenyl)propanehydrazonoyl Chloride (21h) Orange powder (yield 75%), mp 236°C; IR (KBr, *v* cm⁻¹): 3481–3246 (3NH), 1696 (C=O) and 1597 (C=N); ¹H-NMR (DMSO-d_6) δ ppm: 2.38 (s, 3H, CH₃), 7.05 (m, 1H, Ar-H), 7.47 (d, *J*=8.25 Hz, 1H, H⁴ of furan), 7.57 (d, *J*=8.5 Hz, 2H, Ar-H), 7.81 (s, D2O exch., 1H, SO₂NH-), 7.91 (d, *J*=8.25 Hz, 1H, H⁵ of furan), 7.95 (d, *J*=8.5 Hz, 2H, Ar-H), 8.51 (d, *J*=7.0 Hz, 2H, Ar-H), 10.69 (s, D₂O exch., 1H, =NNH–), 11.00 and 11.62 (s, D₂O exch., 1H, –CONH–); ¹³C-NMR (DSMO-d_6) δ ppm: 25.92, 113.80, 114.83, 116.24, 125.53, 129.00, 129.96, 132.25, 133.82, 146.59, 147.42, 157.42, 157.48, 158.82, 188.62; MS *m/z* [%]: 506 [M⁺, 2.4], 64 [100].

Synthesis of Target Compounds 22a–e The sulfone derivatives **20a–e** (1 mmol) was added to a suspension of the 5-nitrofuran-2-carbohydrazide **11** (1 mmol) in absolute ethanol (10 mL), and glacial acetic acid (0.5 mL) was added to the mixture. The reaction mixture refluxed for 0.5 h. The precipitate formed was collected by filtration while hot, washed with hot ethanol, dried and crystallized from EtOH/DMF to afford compounds **22a–e**.

(E)-5-Nitro-N′-(1-phenyl-2-(phenylsulfonyl)ethylidene)furan-2-carbohydrazide (22a) Yellow powder (yield 75%), mp 233°C; IR (KBr, *v* cm⁻¹): 3420, 3278 (2NH), 1700 (C=O), 1591 (C=N) and 1354, 1150 (SO₂); ¹H-NMR (DMSO-d_6) δ ppm: 5.36 and 5.44 (s, 2H, CH₂), 7.40–7.91 (m, 12H, ArH), 11.14 and 11.66 (s, D₂O exch., 1H, –CONH–); MS *m/z* [%]: 414 [(M+1)⁺, 1.1], 413 [M⁺, 3.2], 272 [100].

(E)-N′-(1-(4-Fluorophenyl)-2-(Phenylsulfonyl)ethylidene)-5-nitrofuran-2-carbohydrazide (22b) Yellow powder (yield 75%), mp 255°C; IR (KBr, *v* cm⁻¹): 3419, 3284 (2NH), 1700 (C=O), 1590 (C=N) and 1307, 1154 (SO₂); ¹H-NMR (DMSO-d_6) δ ppm: 5.36 and 5.46 (s, 2H, CH₂), 7.22–7.89 (m, 11H, ArH), 11.13 and 11.67 (s, D₂O exch., 1H, –CONH–); MS *m/z* [%]: 432 [(M+1)⁺, 1.6], 431 [M⁺, 5.0], 290 [100].

(E)-N′-(1-(4-Chlorophenyl)-2-(phenylsulfonyl)ethylidene)-5-nitrofuran-2-carbohydrazide (22c) Yellow powder (yield 75%), mp 223°C; IR (KBr, *v* cm⁻¹): 3414, 3289 (2NH), 1697 (C=O), 1592 (C=N) and 1353, 1153 (SO₂); ¹H-NMR (DMSO-d_6) δ ppm: 5.36 and 5.45 (s, 2H, CH₂), 7.46–7.97 (m, 11H, ArH), 11.14 and 11.67 (s, D₂O exch., 1H, –CONH–); ¹³C-NMR (DSMO-d_6) δ ppm: 62.70, 114.50, 119.00, 128.48, 128.66, 128.80, 129.34, 129.55, 129.70, 131.42, 134.51, 134.88, 139.84, 152.49, 188.62; MS *m/z* [%]: 449 [(M+2)⁺, 2.6], 447 [M⁺, 6.0], 139 [100].

(E)-5-Nitro-N′-(1-(4-nitrophenyl)-2-tosylethylidene)fu-

ran-2-carbohydrazide (22d) Yellow powder (yield 75%), mp 203°C; IR (KBr, v cm^{-1}): 3420, 3288 (2NH), 1680 (C=O), 1595 (C=N) and 1347, 1152 (SO$_2$); ^{1}H-NMR (DMSO-d_6) δ ppm: 2.29 (s, 3H, CH$_3$), 5.41 (s, 2H, CH$_2$), 7.34 (d, J=8.0 Hz, 1H, H^4 of furan), 7.43 (d, J=7.0 Hz, 2H, Ar-H), 7.76 –8.07 (m, 3H, ArH), 8.18 (d, J=7.75 Hz, 2H, Ar-H), 8.32 (d, J=7.75 Hz, 2H, Ar-H), 11.13 and 11.61 (s, D$_2$O exch., 1H, –CONH–); ^{13}C-NMR (DSMO-d_6) δ ppm: 21.40, 63.30, 123.80, 124.19, 128.57, 128.75, 129.03, 130.18, 130.93, 136.10, 136.80, 140.62, 145.30, 150.80, 154.00, 189.03; MS m/z [%]: 472 [M$^+$, 0.6], 140 [100].

(Z)-5-Nitro-N′-(2-(phenylsulfonyl)-1-(thiophen-2-yl)ethylidene)furan-2-carbohydrazide (22e) Yellow powder (yield 75%), mp 140–150°C; IR (KBr, v cm^{-1}): 3414, 3292 (2NH), 1700 (C=O), 1559 (C=N) and 1412, 1158 (SO$_2$); ^{1}H-NMR (DMSO-d_6) δ ppm: 5.25 (s, 2H, CH$_2$), 7.25–8.10 (m, 10H, ArH), 11.13 and 11.61 (s, D$_2$O exch., 1H, –CONH–); ^{13}C-NMR (DSMO-d_6) δ ppm: 63.04, 128.53, 128.73, 129.48, 129.70, 134.54, 137.11, 137.76, 139.73, 143.58, 181.77; MS m/z [%]: 420 [(M+1)$^+$, 2.7], 419 [M$^+$, 10.1], 109 [100].

Synthesis of Hydrazones 23a–g To a stirred solution of the appropriate 2-oxo-N′-(4-substitutedphenyl)-propanehydrazonoyl chloride **16a–e**, **i**, **j** (5 mmol) in THF (20 mL), thiophene-2-carbohydrazide **12** (5 mmol) was added. The reaction mixture was heated under reflux for 10 h. The solid product obtained upon cooling was filtered off and recrystallized from dioxan to afford the corresponding hydrazones **23a–g** with 65–80% yield.

(1Z,2E)-N′-Phenyl-2-(2-(thiophene-2-carbonyl)hydrazono)propanehydrazonoyl Chloride (23a) Yellow powder (yield 75%), mp 220°C; IR (KBr, v cm^{-1}): 3414, 3325 (2NH), 1636 (C=O) and 1598 (C=N); ^{1}H-NMR (DMSO-d_6) δ ppm: 2.38 (s, 3H, CH$_3$), 6.93–7.95 (m, 8H, ArH), 10.18 (s, D$_2$O exch., 1H, =NNH–), 11.00 (s, D$_2$O exch., 1H, –CONH–); ^{13}C-NMR (DSMO-d_6) δ ppm: 13.95, 114.31 (2C), 121.65, 123.81, 127.63, 129.62, 134.56 (2C), 135.32, 143.96, 152.00; MS m/z [%]: 322 [(M+2)$^+$, 3.7], 320 [M$^+$, 9.5], 284 [100].

(1Z,2E)-N′-(4-Fluorophenyl)-2-(2-(thiophene-2-carbonyl)hydrazono)propanehydrazonoyl Chloride (23b) Yellow powder (yield 75%), mp 225°C; IR (KBr, v cm^{-1}): 3420, 3312 (2NH), 1653 (C=O) and 1592 (C=N); ^{1}H-NMR (DMSO-d_6) δ ppm: 2.37 (s, 3H, CH$_3$), 7.13–8.20 (m, 7H, ArH), 10.22 (s, D$_2$O exch., 1H, =NNH–), 11.00 (s, D$_2$O exch., 1H, –CONH–); ^{13}C-NMR (DMSO-d_6) δ ppm: 13.98, 115.56 ($^3J_{F-C}$=7.5 Hz), 116.09 ($^2J_{F-C}$=22.5 Hz), 123.81, 126.50, 127.57 (2C), 133.00, 135.32 (2C), 140.61, 156.73 ($^1J_{F-C}$=235 Hz); MS m/z [%]: 340 [(M+2)$^+$, 1.9], 338 [M$^+$, 4.9], 111 [100].

(1Z,2E)-N′-(4-Chlorophenyl)-2-(2-(Thiophene-2-carbonyl)hydrazono)propanehydrazonoyl Chloride (23c) Yellow powder (yield 75%), mp 230°C; IR (KBr, v cm^{-1}): 3419, 3320 (2NH), 1655 (C=O) and 1586 (C=N); ^{1}H-NMR (DMSO-d_6) δ ppm: 2.38 (s, 3H, CH$_3$), 7.24–8.20 (m, 7H, ArH), 10.29 (s, D$_2$O exch., 1H, =NNH–), 11.02 (s, D$_2$O exch., 1H, –CONH–); ^{13}C-NMR (DSMO-d_6) δ ppm: 14.00, 115.86 (2C), 116.50 (2C), 124.63, 125.13, 127.60, 129.44, 135.26 (3C), 143.00, 154.00; MS m/z [%]: 356 [(M+2)$^+$, 2.3], 354 [M$^+$, 3.4], 111 [100].

(1Z,2E)-N′-(4-Bromophenyl)-2-(2-(thiophene-2-carbonyl)hydrazono)propanehydrazonoyl Chloride (23d) Yellow powder (yield 75%), mp 224°C; IR (KBr, v cm^{-1}): 3414, 3316 (2NH), 1663 (C=O) and 1582 (C=N); ^{1}H-NMR

(DMSO-d_6) δ ppm: 2.37 (s, 3H, CH$_3$), 7.23 (d, J=3.0 Hz, 1H, H^4 of thiophene), 7.31 (d, J=7.25 Hz, 2H, Ar-H), 7.45 (d, J=7.25 Hz, 2H, Ar-H), 7.95–8.20 (m, 2H, H^3 and H^5 of thiophene), 10.33 (s, D$_2$O exch., 1H, =NNH–), 11.02 (s, D$_2$O exch., 1H, –CONH–); MS m/z [%]: 402 [(M+2)$^+$, 0.7], 400 [M$^+$, 2.7], 111 [100].

(1Z,2E)-N′-(4-Iodophenyl)-2-(2-(thiophene-2-carbonyl)hydrazono)propanehydrazonoyl Chloride (23e) Orange powder (yield 75%), mp 178°C; IR (KBr, v cm^{-1}): 3420, 3320 (2NH), 1652 (C=O) and 1586 (C=N); ^{1}H-NMR (DMSO-d_6) δ ppm: 2.40 (s, 3H, CH$_3$), 7.10–7.91 (m, 7H, ArH), 10.08 and 10.25 (s, D$_2$O exch., 1H, =NNH–), 10.83 (s, D$_2$O exch., 1H, –CONH–); ^{13}C-NMR (DSMO-d_6) δ ppm: 14.31, 114.29, 114.47, 123.21, 128.73, 129.15, 130.02, 130.36, 132.02, 134.29, 141.57, 154.48; MS m/z [%]: 446 [M$^+$, 0.3], 111 [105].

(1Z,2E)-2-(2-(Thiophene-2-carbonyl)hydrazono)-N′-p-tolylpropanehydrazonoyl Chloride (23f) Yellow powder (yield 75%), mp 221°C; IR (KBr, v cm^{-1}): 3420, 3316 (2NH), 1652 (C=O) and 1558 (C=N); ^{1}H-NMR (DMSO-d_6) δ ppm: 2.25 (s, 3H, CH$_3$), 2.37 (s, 3H, CH$_3$), 7.10 (d, J=7.50 Hz, 2H, Ar-H), 7.15–8.21 (m, 5H, ArH), 10.09 (s, D$_2$O exch., 1H, =NNH–), 10.98 (s, D$_2$O exch., 1H, –CONH–); ^{13}C-NMR (DSMO-d_6) δ ppm: 13.97, 20.77, 114.32 (2C), 115.32, 123.18, 127.58, 130.02 (2C), 130.39, 135.30, 141.71 (2C); MS m/z [%]: 336 [(M+2)$^+$, 4.1], 334 [M$^+$, 10.6], 111 [100].

(1Z,2E)-N′-(4-Methoxyphenyl)-2-(2-(thiophene-2-carbonyl)hydrazono)propanehydrazonoyl Chloride (23g) Yellow powder (yield 75%), mp 229°C; IR (KBr, v cm^{-1}): 3421, 3319 (2NH), 1654 (C=O) and 1564 (C=N); ^{1}H-NMR (DMSO-d_6) δ ppm: 2.36 (s, 3H, CH$_3$), 3.72 (s, 3H, OCH$_3$), 6.90 (d, J=8.5 Hz, 2H, Ar-H), 7.23–7.30 (m, 3H, H^4 thiophene +2 Ar-H), 7.95–8.25 (m, 2H, H^3 and H^5 thiophene), 10.05 (s, D$_2$O exch., 1H, =NNH–), 10.95 (s, D$_2$O exch., 1H, –CONH–); ^{13}C-NMR (DSMO-d_6) δ ppm: 13.94, 55.73, 114.98 (2C), 115.47 (2C), 122.59, 127.55, 135.28, 137.77 (2C), 154.66.

Antimicrobial Activity All strains were provided from culture collection of the Regional Center for Mycology and Biotechnology (RCMB), Al-Azhar University, Cairo, Egypt. Antibacterial and antifungal activities were expressed as the diameter of inhibition zones; agar well diffusion method was used. Holes (1 cm diameter) were digger in the agar using sterile cork borer in sterile malt agar plates for fungi and sterile nutrient agar plates for bacteria, which had previously been uniformly seeded with tested microorganisms. The holes were filled by fungal filtrates (100 μL). Plates were left in a cooled incubator at 4°C for one hour for diffusion and then incubated at 37°C for tested bacteria and 28°C for tested fungi. Inhibition zones developed due to active antimicrobial metabolites were measured after 24 h of incubation for bacteria and 48 h of incubation for fungi. Amphotericin B and ciprofloxacin were used as antifungal and antibacterial positive control; respectively. The experiment was performed in triplicate and the average zone of inhibition was calculated.

Minimum Inhibitory Concentration MIC was performed by a serial dilution technique described by Irobi *et al.*,[53] starting with 100 mmol concentration of all compounds dissolved in 1 mL DMSO and then reduced by successive two-fold dilutions of stock solution using a calibrated micropipette. Amphotericin B and ciprofloxacin were used as the reference compounds for fungi and bacteria; respectively. The final solutions concentrations were 125, 62.50, 31.25, 15.63, 7.81, 3.90,

1.95, 0.98, 0.49, 0.24, 0.12 and 0.06 μmol/mL. The microtiter plates were incubated at 37°C for tested bacteria and 28°C for tested fungi and were readied using microplate reader after 24 h for bacteria and after 48 h for fungi. In each case, triplicate tests were performed and the average was taken as final reading. MIC was expressed as the lowest concentration inhibiting test organism's growth.[54]

Antimycobacterial Activity *M. tuberculosis* (RCMB 010126) strain was provided from culture collection of the Regional Center for Mycology and Biotechnology (RCMB), Al-Azhar University, Cairo, Egypt. The isolated *M. tuberculosis* (RCMB 010126) clone was cultivated under agitation on LB medium at 37°C for 24 h. The antitubercular activity was expressed as the diameter of inhibition zones using agar well diffusion method and as MIC using serial dilution technique. Isoniazide and pyrazinamide were used as the reference drugs. The final solutions concentrations were 125, 62.50, 31.25, 15.63, 7.81, 3.90, 1.95, 0.98, 0.49, 0.24 and 0.12 μmol/mL. The zones of inhibition were analyzed after 72 h of incubation at 37°C. Each test was repeated 3 times. MIC was expressed as the lowest concentration inhibiting test organism's growth.

***In Vitro* Cytotoxicity** MDA-MB231 cells were grown in Dulbecco's modified Eagle's medium (DMEM)/high glucose supplemented with 10% fetal bovine serum (FBS), 2 mM L-glutamine and 1% penicillin/streptomycin. The new compounds were evaluated in a primary five cell line-one concentration (25 mg/mL) anticancer assay against MDA-MB231 cells cell lines. The cytotoxic effect of the newly synthesized compounds was evaluated by testing the capacity of the reducing enzymes present in viable cells to convert MTT to formazan crystals as previously described,[55] with some modifications. Briefly, cells cultured in complete medium were seeded into 96-well microtiter plates (in quintuplicates) with 2×10^4 cells per well and incubated at 37°C under a humidified atmosphere of 5% CO_2 for 24 h. The cell medium in test wells were then changed to serum free medium (SFM) containing 25 mg/mL of the test compounds, while the cell medium in control wells were changed to SFM containing an equivalent volume of solvent (dimethyl sulfoxide "DMSO"). After incubation at 37°C for 24 h, SFM in control and test wells were replaced by 100 mL/well of MTT; 0.5 mg/mL) in phosphate-buffered saline (PBS) and incubated at 37°C for an additional 3 h. MTT solution were removed and the purple formazan crystals formed at the bottom of the wells were dissolved using 100 mL isopropyl alcohol/well with shaking for 1 h at room temperature. The absorbance at 549 nm was read on a microplate reader (ELX 800; Bio-Tek Instruments, Winooski, VT, U.S.A.). The dose response curves of the compounds effecting >50% inhibition in one-dose prescreening for each cell line were established with concentrations of 25, 12.5, 6.25, 3.125, 1.56 and 0.78 mg/mL, and the concentrations causing 50% cell growth inhibition (IC_{50}) were calculated.

Molecular Docking The molecular docking of the tested compounds was performed using Discovery Studio 4/CDOCKER protocol (Accelrys Software Inc.). The protein crystallographic structure of *Bacillus anthracis* dihydropteroate synthase (PDB code 3TYE) was downloaded from the Protein Data Bank (PDB). The protein was prepared for docking process according to the standard protein preparation procedure integrated in Accelry's discovery studio 4 and prepared by prepare protein protocol. Sulfathiazole-6-hydroxy-methyl-7,8-dihydropterin-pyrophosphate (STZ-DHPP) adduct and the **21f** were drawn as a database and prepared by prepare ligand protocol to generate 3D structure and refine using CHARMM force field with full potential. Docking simulations were run using CDOCKER protocol where a maximum bad orientations was 800 and orientation van der Waals (vdW) energy threshold was 300. Simulated annealing simulation would be then carried out consisting of a heating phase 700 K with 2000 steps and a cooling phase back to 5000 steps. The binding energy was calculated as a score to rank the docking poses. The top 10 docking poses would be finally saved. Docking poses were ranked according to their –CDOCKER interaction energy, and the top poses were chosen for analysis of interactions for each compound.

Conflict of Interest The authors declare no conflict of interest.

REFERENCES

1) Choffnes E, Relman D, Mack A. Antibiotic Resistance: Implications for Global Health and Novel Intervention Strategies. *Workshop Summary*, The National Academies Press, Washington, D.C. (2010).
2) Wright GD. Antibiotics: a new hope. *Chem. Biol.*, **19**, 3–10 (2012).
3) Heymann DL. Resistance to anti-infective drugs and the threat to public health. *Cell*, **124**, 671–675 (2006).
4) Coates A, Hu Y, Bax R, Page C. The future challenges facing the development of new antimicrobial drugs. *Nat. Rev. Drug Discov.*, **1**, 895–910 (2002).
5) Demain AL. Antibiotic discovery: a step in the right direction. *Chem. Biol.*, **18**, 939 (2011).
6) Lewis K. Platforms for antibiotic discovery. *Nat. Rev. Drug Discov.*, **12**, 371–387 (2013).
7) Payne DJ, Gwynn MN, Holmes DJ, Pompliano DL. Drugs for bad bugs: confronting the challenges of antibacterial discovery. *Nat. Rev. Drug Discov.*, **6**, 29–40 (2007).
8) Kedderis GL, Miwa GT. The metabolic activation of nitroheterocyclic therapeutic agents. *Drug Metab. Rev.*, **19**, 33–62 (1988).
9) Jorge SD, Masunari A, Rangel-Yagui CO, Pasqualoto KF, Tavares LC. Design, synthesis, antimicrobial activity and molecular modeling studies of novel benzofuroxan derivatives against *Staphylococcus aureus*. *Bioorg. Med. Chem.*, **17**, 3028–3036 (2009).
10) Viodé C, Bettache N, Cenas N, Krauth-Siegel RL, Chauviere G, Bakalara N, Perie J. Enzymatic reduction studies of nitroheterocycles. *Biochem. Pharmacol.*, **57**, 549–557 (1999).
11) Leonard F, Andremont A, Tancrede C. *In vivo* activity of nifurzide and nifuroxazide in intestinal bacteria in man and gnotobiotic mice. *J. Appl. Bacteriol.*, **58**, 545–553 (1985).
12) Dougherty TJ, Pucci MJ. *Antibiotic discovery and development*. Springer, New York (2012).
13) Vass M, Hruska K, Franek M. Nitrofuran antibiotics: a review on the application, prohibition and residual analysis. *Vet. Med.*, **53**, 469–500 (2008).
14) Zhou L, Stewart G, Rideau E, Westwood NJ, Smith TK. A class of 5-nitro-2-furancarboxylamides with potent trypanocidal activity against *Trypanosoma brucei in vitro*. *J. Med. Chem.*, **56**, 796–806

(2013).

15) Hofnung M, Quillardet P, Michel V, Touati E. Genotoxicity of 2-nitro-7-methoxy-naphtho[2,1-*b*]furan (R7000): a case study with some considerations on nitrofurantoin and nifuroxazide. *Res. Microbiol.*, **153**, 427–434 (2002).

16) Kamal A, Hussaini SM, Faazil S, Poornachandra Y, Narender Reddy G, Kumar CG, Rajput VS, Rani C, Sharma R, Khan IA, Jagadeesh Babu N. Anti-tubercular agents. Part 8: synthesis, antibacterial and antitubercular activity of 5-nitrofuran based 1,2,3-triazoles. *Bioorg. Med. Chem. Lett.*, **23**, 6842–6846 (2013).

17) Badr SM, Barwa RM. Synthesis of some new [1,2,4]triazolo[3,4-*b*][1,3,4]thiadiazines and [1,2,4]triazolo[3,4-*b*][1,3,4]thiadiazoles starting from 5-nitro-2-furoic acid and evaluation of their antimicrobial activity. *Bioorg. Med. Chem.*, **19**, 4506–4512 (2011).

18) Zorzi RR, Jorge SD, Palace-Berl F, Pasqualoto KF, Bortolozzo Lde S, de Castro Siqueira AM, Tavares LC. Exploring 5-nitrofuran derivatives against nosocomial pathogens: synthesis, antimicrobial activity and chemometric analysis. *Bioorg. Med. Chem.*, **22**, 2844–2854 (2014).

19) Masunari A, Tavares LC. A new class of nifuroxazide analogues: synthesis of 5-nitrothiophene derivatives with antimicrobial activity against multidrug-resistant *Staphylococcus aureus*. *Bioorg. Med. Chem.*, **15**, 4229–4236 (2007).

20) Pires JR, Saito C, Gomes SL, Giesbrecht AM, Amaral AT. Investigation of 5-nitrofuran derivatives: synthesis, antibacterial activity, and quantitative structure–activity relationships. *J. Med. Chem.*, **44**, 3673–3681 (2001).

21) Khalil AM, Berghot MA, Gouda MA. Synthesis and antibacterial activity of some new thiazole and thiophene derivatives. *Eur. J. Med. Chem.*, **44**, 4434–4440 (2009).

22) Nasr T, Bondock S, Eid S. Design, synthesis, antimicrobial evaluation and molecular docking studies of some new thiophene, pyrazole and pyridone derivatives bearing sulfisoxazole moiety. *Eur. J. Med. Chem.*, **84**, 491–504 (2014).

23) Stolic I, Cipcic Paljetak H, Peric M, Matijasic M, Stepanic V, Verbanac D, Bajic M. Synthesis and structure–activity relationship of amidine derivatives of 3,4-ethylenedioxythiophene as novel antibacterial agents. *Eur. J. Med. Chem.*, **90**, 68–81 (2015).

24) Schuch R, Pelzek AJ, Raz A, Euler CW, Ryan PA, Winer BY, Farnsworth A, Bhaskaran SS, Stebbins CE, Xu Y, Clifford A, Bearss DJ, Vankayalapati H, Goldberg AR, Fischetti VA. Use of a bacteriophage lysin to identify a novel target for antimicrobial development. *PLoS ONE*, **8**, e60754 (2013).

25) Tavares LC, Chiste JJ, Santos MG, Penna TC. Synthesis and biological activity of nifuroxazide and analogs. II. *Boll. Chim. Farm.*, **138**, 432–436 (1999).

26) De Logu A, Onnis V, Saddi B, Congiu C, Schivo ML, Cocco MT. Activity of a new class of isonicotinoylhydrazones used alone and in combination with isoniazid, rifampicin, ethambutol, *para*-aminosalicylic acid and clofazimine against *Mycobacterium tuberculosis*. *J. Antimicrob. Chemother.*, **49**, 275–282 (2002).

27) Hearn MJ, Cynamon MH, Chen MF, Coppins R, Davis J, Joo-On Kang H, Noble A, Tu-Sekine B, Terrot MS, Trombino D, Thai M, Webster ER, Wilson R. Preparation and antitubercular activities *in vitro* and *in vivo* of novel Schiff bases of isoniazid. *Eur. J. Med. Chem.*, **44**, 4169–4178 (2009).

28) Aboul-Fadl T, Mohammed FA, Hassan EA. Synthesis, antitubercular activity and pharmacokinetic studies of some Schiff bases derived from 1-alkylisatin and isonicotinic acid hydrazide (INH). *Arch. Pharm. Res.*, **26**, 778–784 (2003).

29) Abdel-Aziza HA, Abdel-Wahab BF, Badria FA. Stereoselective synthesis and antiviral activity of (1*E*,2*Z*,3*E*)-1-(piperidin-1-yl)-1-(arylhydrazono)-2-[(benzoyl/benzothiazol-2-oyl)hydrazono]-4-(aryl(1))but-3-enes. *Arch. Pharm.*, **343**, 152–159 (2010).

30) Abdel-Aziz HA, Mekawey AA. Stereoselective synthesis and antimicrobial activity of benzofuran-based (1*E*)-1-(piperidin-1-yl)-N2-

arylamidrazones. *Eur. J. Med. Chem.*, **44**, 4985–4997 (2009).

31) Abdel-Wahab BF, Abdel-Aziz HA, Ahmed EM. Convenient synthesis and antimicrobial activity of new 3-substituted 5-(benzofuran-2-yl)-pyrazole derivatives. *Arch. Pharm.*, **341**, 734–739 (2008).

32) Ghabbour HA, Qabeel MM, Eldehna WM, Al-Dhfyan A, Abdel-Aziz HA. Design, synthesis, and molecular docking of 1-(1-(4-chlorophenyl)-2-(phenylsulfonyl)ethylidene)-2-phenylhydrazine as potent nonazole anticandidal agent. *Journal of Chemistry*, **2014**, 1–8 (2014).

33) Ibrahim HS, Eldehna WM, Abdel-Aziz HA, Elaasser MM, Abdel-Aziz MM. Improvement of antibacterial activity of some sulfa drugs through linkage to certain phthalazin-1(2*H*)-one scaffolds. *Eur. J. Med. Chem.*, **85**, 480–486 (2014).

34) Sriram D, Yogeeswari P, Devakaram RV. Synthesis, *in vitro* and *in vivo* antimycobacterial activities of diclofenac acid hydrazones and amides. *Bioorg. Med. Chem.*, **14**, 3113–3118 (2006).

35) Shawali AS, Farghal TA. Reactions of hydrazonoyl halides with heterocyclic thiones. Convenient methodology for heteroannulation, synthesis of spiroheterocycles and heterocyclic ring transformation. *ARKIVOC*, **2008**, 18–64 (2008).

36) King LC, Ostrum GK. Selective bromination with copper(II) bromide. *J. Org. Chem.*, **29**, 3459–3461 (1964).

37) Swenson RE, Sowin TJ, Zhang HQ. Synthesis of substituted quinolines using the dianion addition of *N*-Boc-anilines and alpha-tolylsulfonyl-alpha,beta-unsaturated ketones. *J. Org. Chem.*, **67**, 9182–9185 (2002).

38) Padmavathi V, Reddy SN, Mahesh K. Synthesis, antimicrobial and antioxidant activities of sulfone linked bis heterocycles-pyrazolyl oxadiazoles and pyrazolyl thiadiazole. *Chem. Pharm. Bull.*, **57**, 1376–1380 (2009).

39) Muralikrishna A, Venkatesh BC, Padmavathi V, Padmaja A, Kondaiah P, Krishna NS. Synthesis, antimicrobial and cytotoxic activities of sulfone linked bis heterocycles. *Eur. J. Med. Chem.*, **54**, 605–614 (2012).

40) Yamasaki M, Harada E, Tamura Y, Lim SY, Ohsuga T, Yokoyama N, Morishita K, Nakamura K, Ohta H, Takiguchi M. *In vitro* and *in vivo* safety and efficacy studies of amphotericin B on *Babesia gibsoni*. *Vet. Parasitol.*, **205**, 424–433 (2014).

41) Dagenais TR, Keller NP. Pathogenesis of *Aspergillus fumigatus* in invasive aspergillosis. *Clin. Microbiol. Rev.*, **22**, 447–465 (2009).

42) Morikawa H, Tomishima M, Kayakiri N, Araki T, Barrett D, Akamatsu S, Matsumoto S, Uchida S, Nakai T, Takeda S, Maki K. Synthesis and antifungal activity of ASP9726, a novel echinocandin with potent *Aspergillus hyphal* growth inhibition. *Bioorg. Med. Chem. Lett.*, **24**, 1172–1175 (2014).

43) Orme I, Tuberculosis Drug Screening Program. Search for new drugs for treatment of tuberculosis. *Antimicrob. Agents Chemother.*, **45**, 1943–1946 (2001).

44) Krátký M, Vinsova J, Volkova M, Buchta V, Trejtnar F, Stolarikova J. Antimicrobial activity of sulfonamides containing 5-chloro-2-hydroxybenzaldehyde and 5-chloro-2-hydroxybenzoic acid scaffold. *Eur. J. Med. Chem.*, **50**, 433–440 (2012).

45) Argyropoulou I, Geronikaki A, Vicini P, Zanib F. Synthesis and biological evaluation of sulfonamide thiazole and benzothiazole derivatives as antimicrobial agents. *ARKIVOC*, **2009**, 89–112 (2009).

46) Yun MK, Wu Y, Li Z, Zhao Y, Waddell MB, Ferreira AM, Lee RE, Bashford D, White SW. Catalysis and sulfa drug resistance in dihydropteroate synthase. *Science*, **335**, 1110–1114 (2012).

47) Kier LB, Hall LH. *Molecular connectivity indices in chemistry and drug research*. Academic Press, New York (1976).

48) Kier LB, Hall LH. *Molecular connectivity in structure–activity analysis*. Research Studies Press Ltd., New York (1985).

49) Bonchev D. *Information theoretic indices for characterization of chemical structures*. Research Studies Press Ltd., New York (1983).

50) Hall L, Mohney B, Kier L. The electrotopological state: structure information at the atomic level for molecular graphs. *J. Chem. Inf.*

Comput. Sci., **31**, 76–82 (1991).

51) Hall LH, Kier LB. The E-state as the basis for molecular structure space definition and structure similarity. *J. Chem. Inf. Comput. Sci.*, **40**, 784–791 (2000).

52) Stanton DTJ, Jurs PC. P.C.: Development and use of charge partial surface area structural descriptors in computer-assisted quantitative structure–property relationship studies. *Anal. Chem.*, **62**, 2323–2329 (1990).

53) Irobi ON, Moo-Young M, Anderson WA. Antimicrobial activity of annatto (*Bixa orellana*) extract. *Pharmaceutical Biology*, **34**, 87–90 (1996).

54) Urzua A, Caroli M, Vasquez L, Mendoza L, Wilkens M, Tojo E. Antimicrobial study of the resinous exudate and of diterpenoids isolated from *Eupatorium salvia* (Asteraceae). *J. Ethnopharmacol.*, **62**, 251–254 (1998).

55) Köhle C, Badary OA, Nill K, Bock-Hennig BS, Bock KW. Serotonin glucuronidation by Ah receptor- and oxidative stress-inducible human UDP-glucuronosyltransferase (UGT) 1A6 in Caco-2 cells. *Biochem. Pharmacol.*, **69**, 1397–1402 (2005).